分散から凝集へのクロスオーバーでの細胞認識による集団細胞運動

松下勝義, 新垣大幸, 鎌本直也, 須藤麻希, 藤本仰一

阪大院理 生物

概要

我々は細胞の集団運動における分散状態と凝集状態の遷移の効果を調べた. 我々は細胞間で相互に認識して運動する高濃度の細胞系を細胞 Potts 模型で考え, 細胞の運動方向の秩序を計算した. そして我々は平衡系では不連続に起きる分散と凝集状態の間の遷移であっても集団運動化は連続的に起きることを示した. これは集団運動の細胞の相互誘導のみでは説明できず, 何らかの別の知られていない非平衡効果の存在が予想される.

Collective Cell Movement through Cell Sensing in Crossover from Suspended to Aggregated States

Katsuyoshi Matsushita, Taiko Arakaki, Naoya Kamamoto, Maki Sudo, and Koichi Fujimoto

Department of Biological Science, Graduate School of Science, Osaka University.

Abstract

We investigate the effect of the transition between the suspended and aggregated states on collective cell movement. We consider high-density cells in the cellular Potts model with sensing cells as a trigger to move. Based on this model, we evaluate the order of the cell moving direction. We show that the crossover to the order from disorder occurs gradually even though the transition without the sensing occurs abruptly. This gradual crossover partially reflects the characteristics of cell sensing.

1 Introduction

Collective movements of cells are indispensable to the development of eukaryotes [1–3]. In this collective movement, cells sense each other through their mechanical contacts and use this as a trigger to move. In addition, cells aggregate depending on developmental stages, organs, and species by using intercellular adhesions. This aggregation enables cells to sense each other through their contacts easily. Therefore, the collective movement due to the sensing inevitably reflects the aggregation condition. The effect of this condition on the collective movement should be clarified to promote our understanding of this movement.

To consider the effect in the collective movement, we briefly introduce the effect for the case without the movement and then consider its application to the case with the movement. In the case without the movement, the following condition for surface tensions is known as the aggregation condition [4],

$$\gamma_{\mathrm{E}} > \gamma_{\mathrm{C}}/2, \tag{1}$$

where γ_{C} is the surface tension between cells, including the effect of the intercellular adhesion. γ_{E} is that between cells and medium. This condition results from the fact that two interfaces between two cells and a medium should form to separate two adhesive contacting cells. At $\gamma_{\mathrm{E}} = \gamma_{\mathrm{C}}/2$, this effect of the interface tensions drives the transition between the suspended and aggregated states. There, we can expect that the collective movement switches abruptly.

We consider the applicability of this condition to the case with the movement through the cell sensing. In this case, cells effectively reduce γ_{C} on their leading edge to move with sensing other cells. Inevitably, we should consider that the reduction directions of γ_{C} adjusted to relax in the aggregation. This adjustment makes the simple application of the aggregation condition difficult. Therefore, we should investigate the effect of the transition between the suspended (individual cell) and aggregated cells separately from the case without movement.

The transition reflects the cell density and the interface tension between cells and the medium. Because these are not easily controllable in experiments, using a theoretical model helps us understand this transition. Here, we investigate this

transition using a theoretical model. In particular, we focus on the dependence of moving direction ordering on the cell density and the interface tension.

The present work considers the cellular Potts model [4–8] with cell sensing as the theoretical model. We consider a finite periodic system and sufficiently dense cells, where the cells frequently contact and sense each other as a trigger to move. To estimate the ordering of moving direction, we evaluate the motion ordering of driving direction. We find that the motion ordering gradually occurs at the transition. This gradualness is contrast to the abruptness of the aggregation transition without movement.

2 Model

The interface tension between the cells and the medium is an essential control parameter for our analysis. Therefore, we model the interface tension using the cellular Potts model [5] because this model easily controls the tension. This model expresses the cells as a single domain of a Potts state on the lattice. Here, we denote the state by $m(\boldsymbol{r})$ at site $\boldsymbol{r}$ on the square lattice. We consider a square-shaped system with linear size L with the periodic boundary condition. $m(\boldsymbol{r}) = 0$ represents medium and otherwise $m(\boldsymbol{r})$ represents the index of a cell. We denote the number of cells by N and keep it constant. A repetition of a Monte Carlo update of this Potts state, hereafter explained, generates the cell configuration series in the motion of cells.

In the Monte Carlo update, the generated probability of a state is proportional to the Boltzmann weight $w = \exp(-\beta\mathcal{H})$. Here, $\mathcal{H}$ is the free energy and β is the strength of the cell shape fluctuation. The Monte Carlo update gives the time unit of this simulation and consists of $16L^2$ trials. In a trial, we randomly select the site $\boldsymbol{r}$. Then, we probabilistically change its state $m(\boldsymbol{r})$ to be that of a randomly selected neighboring site. The probability of this change is the Metropolis probability $\min[1, w'/w]$. Here, w' is the Boltzmann weight after the update of the state.

$\mathcal{H}$ consists of three free-energy terms

$$\mathcal{H} = \mathcal{H}_{\mathrm{S}} + \mathcal{H}_{\mathrm{A}} + \mathcal{H}_{\mathrm{G}}. \tag{2}$$

The first term consists of the surface tension between cells and that between cell and medium

$$\begin{aligned}\mathcal{H}_{\mathrm{S}} = {} & \gamma_{\mathrm{C}} \sum_{\boldsymbol{r}\boldsymbol{r}'} \eta_{m(\boldsymbol{r})m(\boldsymbol{r}')}\eta_{0m(\boldsymbol{r}')}\eta_{m(\boldsymbol{r})0} \\ & + \gamma_{\mathrm{E}} \sum_{\boldsymbol{r}\boldsymbol{r}'} \eta_{m(\boldsymbol{r})m(\boldsymbol{r}')} \left[\delta_{0m(\boldsymbol{r}')} + \delta_{m(\boldsymbol{r})0}\right].\end{aligned} \tag{3}$$

In the summation, we conventionally take the neighboring site pair $\boldsymbol{r}\boldsymbol{r}'$ over the nearest and next-nearest sites [5]. The definitions of the pair are the same hereafter. γ_{C} is the surface tension between cells, and γ_{E} is that of cell and medium. δ_{nm} is the Kronecker's δ and η_{nm} is $1-\delta_{nm}$. In this study, we control γ_E with N and examine the dependence of the ordering on them.

The second term in Eq. (2) is the volume constraint,

$$\mathcal{H}_{\mathrm{A}} = \kappa A \sum_m (1 - \frac{\sum_{\boldsymbol{r}} \delta_{mm(\boldsymbol{r})}}{A})^2, \tag{4}$$

where κ is compressibility for the occupation area of cells and A is its natural value.

The third term in Eq. (2) is the driving force [9]

$$\mathcal{H}_{\mathrm{G}} = -\delta \sum_{\boldsymbol{r}\boldsymbol{r}'} \eta_{m(\boldsymbol{r})m(\boldsymbol{r}')}\eta_{0m(\boldsymbol{r}')}\eta_{m(\boldsymbol{r})0} \left[\sum_{\boldsymbol{x}\in\{\boldsymbol{r}\boldsymbol{r}'\}} q_{\boldsymbol{x}}^{m(\boldsymbol{x})}\right]. \tag{5}$$

Here, $q_{\boldsymbol{r}}^m = 1 + \boldsymbol{p}_{m(\boldsymbol{r})} \cdot \boldsymbol{e}_{m(\boldsymbol{r})}$ is the potential gradient in the direction of a unit vector $\boldsymbol{p}_m$, which indicates the driving direction. The unit vector $\boldsymbol{e}_m(\boldsymbol{r})$ indicates $\boldsymbol{r}$ from $\boldsymbol{R}_m$, where $\boldsymbol{R}_m$ is the center of the mth cell. $\boldsymbol{p}_m$ and $\boldsymbol{R}_m$ are updated once for each Monte Carlo step with the equation [10]

$$\frac{d\boldsymbol{p}_m}{dt} = \frac{1}{\tau}\left[\frac{d\boldsymbol{R}_m}{dt} - \boldsymbol{p}_m\left(\boldsymbol{p}_m \cdot \frac{d\boldsymbol{R}_m}{dt}\right)\right], \tag{6}$$

and with the replacement of $\boldsymbol{R}_m = \sum_{\boldsymbol{r}} \boldsymbol{r}\delta_{mm(\boldsymbol{r})} / \sum_{\boldsymbol{r}} \delta_{mm(\boldsymbol{r})}$, respectively. Here, t is time, and τ is the relaxation-time ratio of $\boldsymbol{R}_m$ to $\boldsymbol{p}_m$. This setting differs from the self-propulsion [11, 12] and mutual guiding [9, 13] but similarly induces the self-propulsion in the direction of $\boldsymbol{p}_m$ [14]. This propulsion is effectively equivalent to the reduction of the surface tension, mentioned previously.

For this simulation, we set $A = 64$, $\kappa = 64$, $\tau = 5.0$, $\delta = 0.2$, and $\beta = 0.2$ as empirically used for the collective movement. We set γ_E as 4.0; therefore, the abrupt transition from suspended to aggregated states in the case without movement appears at $\gamma_{\mathrm{C}} = 2.0$. We consider γ_{C} from 0.0 to 4.0 to observe the effect of the transition. We solve Eq. (6) by the Euler method with a time difference of $\tau^{-1} = 0.2$, and as mentioned above, the integration is carried out once for each Monte Carlo step. We choose the number of cells $N = 576$ to $N = 854$. $N = 576$ corresponds to the expected value of area fraction $VN/L^2 = 1.0$, where $L = 192$; therefore, the cells in this range of N is expected to cover the whole region of systems in the case without the effect of the interface tension. These numbers enable cell sensing to function effectively through sufficient cellular contacts and promote order in the moving direction.

3 Results and Discussions

At first, we should clarify the dependence of moving direction ordering on γ_E and N for our purpose. Because the moving direction correlates with the

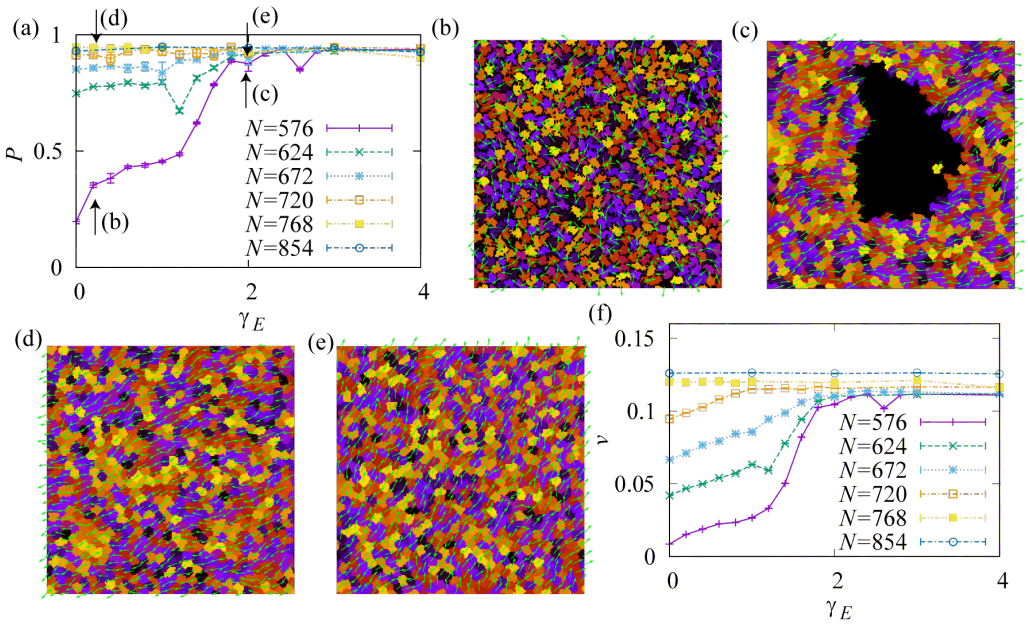

Fig. 1: (a) Order parameter P as a function of the surface tension between cells and a medium $\gamma_{\rm E}$. The data correspond to N = 576, 624, 672, 720, 768, and 854. (b), (c), (d), and (e) show snapshots of cell configuration for N= 576, $\gamma_{\rm E}$ = 0.2; N= 576, $\gamma_{\rm E}$ = 2.0; N= 768, $\gamma_{\rm E}$ = 0.2 and N= 576, $\gamma_{\rm E}$ = 2.0, respectively. In these panels, black regions represent medium and colored regions, cells. The green arrows are the driving direction of each cell. (f) the average velocity v as a function of $\gamma_{\rm E}$.

driving direction $\boldsymbol{p}_m$, the moving direction ordering is detectable by the ordering of $\boldsymbol{p}_m$. Therefore, we calculate the order parameter of $\boldsymbol{p}_m$ [15, 16]

$$P = \left| \int_{t_i}^{t_f+t_i} dt' \frac{1}{N t_f} \sum_m \boldsymbol{p}_m \right|, \qquad (7)$$

to probe the ordering of moving directions. Here, we simulate the relaxation of state during $t_i = 10^4$ updates to obtain the steady state and then calculate P in the period up to $t_f = 10^4$ updates. To examine the ordering of moving direction, we plot P as a function of $\gamma_{\rm E}$ for N from 576 to 854 in Fig. 1(a).

We naively speculate that the moving direction orders near $N \gtrsim 576$ because the value of N is sufficient for covering the whole system, even without aggregation. However, even at $N = 576$, the order parameter P takes small values for low γ_E. The small value implies that the cells inhibit their contacts and cannot sense themselves. As direct evidence of this inhibition, the cell configuration in Fig. 1(b) shows the retainment of the medium between cells and the separation of cells. The arrows in this figure represent the direction of $\boldsymbol{p}_m$ and reflect the disorder in the moving directions, which is consistent with the low value of P. These results show that this high cell density is insufficient for perfect ordering.

As $\gamma_{\rm E}$ increases below $\gamma_{\rm C}/2 \sim 2$ from 1.5, the order parameter gradually increases. This increase indicates that the cells gradually squeeze the medium out with increasing $\gamma_{\rm E}$ and increase the size of their aggregation. Thus, in contrast to an abrupt transition from suspended to aggregated states in our naive speculation, the aggregation gradually progresses as $\gamma_{\rm E}$ increases. The result is not expected from the naive speculation in the case without movement and may be characteristics in the non-equilibrium case.

At high values of $\gamma_{\rm E}$, the cells entirely exclude the medium and form aggregation, as shown in Fig. 1(c). The total area of cells is sufficient for covering the whole system. However, the medium remains by forming a bubble. Therefore, the cells cannot cover the system. The medium remains because the surface tension $\gamma_{\rm E}$ between cells and medium reduces cell area. Namely, the result indicates that the cell density is insufficient for cells to cover the system perfectly under the cell movement, even when the cell density is high enough that the total natural area of cells is equal to that of the system.

In high cell densities, P is independent of $\gamma_{\rm E}$. For example, $N = 768$, P does not depend on the $\gamma_{\rm E}$. As shown in Fig. 1(d) and 1(e), the cells in low and high $\gamma_{\rm E}$ perfectly squeeze the medium out and form a confluent state. Therefore, the cell density is sufficient for cells to cover the entire system. Furthermore, cells exhibit perfect ordering through cell sensing. This density value corresponds to the area fraction of 1.3 and is much higher than our expectation of unity.

The velocity of collective movements reflects the motion order. In Fig. 1(f), we plot the average

velocity of cells to see this,

$$v = \left| \int_{t_i}^{t_i+t_f} \frac{1}{Nt_f} \sum_{m}^{N} \boldsymbol{d}_i \right|, \tag{8}$$

as a function of $\gamma_{\rm E}$ for various N. Here, $\boldsymbol{d}_m$ is the displacement vector of the mth cell. v behaves similarly to P and reflects the ordering of the moving directions.

4 Summary and Remarks

In summary, we consider the transition from the suspended to aggregated states and its effect on the ordering of moving direction due to cell sensing. To examine this effect, we consider sufficient high-density cells at the area fraction of unity, where cells sense each other through forming contacts. We show that the crossover to ordering occurs gradually as interface tension $\gamma_{\rm E}$ increases from the value of suspended cells to that of aggregated cells. This gradualness suggests that a non-equilibrity effect of the collective cell movement induces the gruadual crossover of suspension to aggregation states.

One possible mechanism of this gradual crossover is the effect of the driving force of cells. The effect of the driving force in Eq. (5) is equivalent to reducing the surface tension in the leading edge of cells between them. The value of driving force δ effectively reduces the surface tension by stabilizing the contacts of cells. The reduction of cell-cell surface tension $\gamma_{\rm C}$ is -2$\delta \sim -0.4$ in order states. This effect reduces the transition point to $\gamma_{\rm E} = (\gamma_{\rm C} - 2\delta)/2 \sim 1.8$ in the leading edge of cells. Additionally, the reduction value of surface tension depends on the relative direction of the position of the cellular contacts against the driving direction, as shown in Eq. (5). This direction dependence gives rise to the gradually increase of interface area between cells satisfying the aggregation condition with increasing $\gamma_{\rm E}$. As a result, the reduction gradually promotes the contact formation and stabilizes the order of moving directions through the contacts. Therefore, the driving force qualitatively explains our results.

Regarding the accuracy of the crossover onset of γ_E, we quantitatively overestimate the value $\gamma_{\rm E} \sim 1.8$ compared to the observed value, $\gamma_{\rm E} \sim 1.5$. This overestimation may imply the existence of another non-equilibrium effect.

As an additional remark, we note that $VN/L^2 \sim 1$ is insufficient for the collective movement in the case of small $\gamma_{\rm E}$'s. This insufficiency indicates that the steady state strongly depends on the existence of the medium. For example, the result changes when we choose the state without medium as the initial state. Namely, $\lim_{VN/L^2 \to 1} P$ in the case with a medium is not equivalent to that without a medium. In the case of $VN/L^2 \sim 1$, the initial state without a medium seems to be one of the appropriate states because the cells seemingly cover the whole region of the system. However, our result suggests that the appropriateness depends on the existence of a sufficient amount of the medium. Therefore, we should revisit the investigations in previous works with high-density cells concerning this appropriateness of the initial condition [12, 17, 18] because some of these works assumed the independence of initial conditions.

We thank S. Yabunaka, H. Kuwayama, H. Hashimura, M. Sawada, and K. Sawamoto for providing various relative knowledge. We also thank M. Kikuchi and H. Yoshino for their support with the research resource. This work was supported by JSPS KAKENHI (Grant Number 19K03770) and AMED (Grant Number JP19gm1210007).

References

[1] C. J. Weijer, J. Cell Sci. **122**, 3215 (2015).

[2] P. Friedl and D. Gilmour, Nat. Rev. Mol. Cell Biol. **10**, 445 (2009).

[3] P. Rørth, Annu. Rev. Cell Dev. Biol. **25**, 407 (2009).

[4] J. A. Glazier and F. Graner, Phys. Rev. E **47**, 2128 (1993).

[5] F. Graner and J. A. Glazier, Phys. Rev. Lett. **69**, 2013 (1992).

[6] F. Graner, J. Theor. Biol. **164**, 455 (1993).

[7] A. R. A. Anderson, M. A. J. Chaplain, and K. A. Rejniak, *Single-Cell-Based Models in Biology and Medicine* (Birkhauser Verlag AG, Basel, 2007).

[8] T. Hirashima, E. G. Rens, and R. M. H. Merks, Dev. Growth Differ. **59**, 329 (2017).

[9] K. Matsushita, Phys. Rev. E **97**, 042413 (2018).

[10] B. Szabó, G. J. Szollosi, B. Gonci, Z. Juranyi, D. Selmeczi, and T. Vicsek, Phys. Rev. E **74**, 061908 (2006).

[11] P. Szabó, M. Nagy, and T. Vicsek, Phys. Rev. E **79**, 021908 (2007).

[12] A. J. Kabla, J. R. Soc. Interface **9**, 3268 (2012).

[13] K. Matsushita, Phys. Rev. E **95**, 032415 (2017).

[14] K. Matsushita, Phys. Rev. E **101**, 052410 (2020).

[15] T. Vicsek, A. Czirók, E. Ben-Jacob, I. Cohen, and O. Shochet, Phys. Rev. Lett. **75**, 1226 (1995).

[16] M. C. Marchetti, J. F. Joanny, S. Ramaswamy, T. B. Liverpool, J. Prost, M. Rao, and R. A. Simha, Rev. Mod. Phys. **85**, 1143 (2013).

[17] K. Matsushita, K. Horibe, N. Kamamoto, S. Yabunaka, and K. Fujimoto, Proc. Sympo. Traffic Flow Self-driven Particles **25**, 21 (2019).

[18] K. Matsushita, S. Yabunaka, and K. Fujimoto, J. Phys. Soc. Jpn. **90**, 054801 (2020).

E-mail: kmatsu@bio.sci.osaka-u.ac.jp